Ecological Informatics 10 (2012) 65–72

Contents lists available at SciVerse ScienceDirect

Ecological Informatics

journal homepage: www.elsevier.com/locate/ecolinf

Using digital cameras for comparative phenological monitoring in an evergreen broad-leaved forest and a seasonal rain forest

Junbin Zhao [a,e], Yiping Zhang [a,b,c,*], Zhenghong Tan [a,e], Qinghai Song [a,e], Naishen Liang [d], Lei Yu [a,e], Junfu Zhao [a,e]

[a] Key Lab of Tropical Forest Ecology, Xishuangbanna Tropical Botanical Garden, Chinese Academy of Sciences, Menglun, Yunnan 666303, China
[b] Ailaoshan Station for Subtropical Forest Ecosystem Research, Chinese Ecosystem Research Networks, Jingdong, Yunnan 676209, China
[c] National Forest Ecosystem Research Station at Ailaoshan, Jingdong, Yunnan 676209, China
[d] Center for Global Environmental Research, National Institute for Environmental Studies, Tsukuba, Ibaraki 305-8506, Japan
[e] Graduate University of Chinese Academy of Sciences, Beijing 100049, China

ARTICLE INFO

Article history:
Received 15 April 2011
Received in revised form 1 March 2012
Accepted 2 March 2012
Available online 8 March 2012

Keywords:
Color index
Digital image
Evergreen arboreal forest
Phenological event
Seasonal tropical rain forest
White balance

ABSTRACT

Digital cameras have been used in phenological observations for their high accuracy and low labor cost. Most studies successfully use greenness indices derived from digital images for timing the events related to leaf development. However, when timing the leaf senescence events, wide discrepancies between actual and estimated dates are common. In this study, images of three species (two from an evergreen broad-leaved forest and one from a seasonal rain forest) were used to estimate three phenological events of leaf development and senescence. Other than the greenness index, a redness index was also employed. Different annual patterns in color indices developed among the species. The redness index was more accurate when estimating leaf senescence, while the greenness index was more accurate for estimating leaf development events in *Acer heptalobum* and *Machilus bombycina*. The absolute differences in estimations of phenological events ranged from −3 to 1 day, which is more accurate than estimates based on the greenness index only (−2 to 27 days). With the introduction of the redness index, this technique has been much improved and is possible to be applied to more species. Furthermore, variations of color indices during periods of phenological events were highly related to the climatic factors with a time lag of around 10 days. Because of the ease of use and efficiency (*i.e.*, automatic daily data output), digital cameras are expected to be used in ecosystem process modeling, networks of phenology assessment and validation of the remote sensing results from satellites.

1. Introduction

During the last half century, climate change has shown profound effects on ecosystems all over the globe (Bradshaw and Holzapfel, 2008; Root et al., 2003; Walther et al., 2002). Plant phenology is considered to be a reliable indicator for climate change due to its high sensitivity to climate (Keatley et al., 2002; Kington, 1974; Schwartz, 1990). In response to increasing temperature, many species in temperate regions have exhibited advanced spring phenology (*e.g.*, leaf budburst, leaf flushing and flowering) and delayed autumn senescence (*e.g.*, leaf coloring and leaf shedding), which have led to a prolonged growing season (Chen et al., 2005; Doi and Katano, 2008; Gordo and Sanz, 2009; Matsumoto et al., 2003; Menzel and Fabian, 1999). With the shift of phenology, carbon and water cycles within terrestrial ecosystems have also been altered (Fitzjarrald et al., 2001; Keeling et al., 1996; Niemand et al., 2005; Obrist et al., 2003; Penuelas and Filella, 2001). Therefore, to better understand and simulate these processes at a regional or global scale, widespread phenology observations with standardized rules and skills are needed (Chiang and Brown, 2007).

Phenological observations have been carried out for over a century (Rutishauser et al., 2007). However, in long-term observations, the phenological records are often biased due to different observers (Kharin, 1976; Menzel, 2002). The lack of volunteers also limits the spatial and temporal coverage of phenology assessments. During the last two decades, remote sensing has been used to monitor phenology at regional and global scales. However, due to low accuracy from atmospheric disturbances (Ahl et al., 2006; Zhang et al., 2006), there is still a need to routinely validate many remote sensing simulated assessments from satellites by the ground-based observations (Stockli et al., 2007). Additionally, phenological studies based on remote sensing are usually not species-specific (but in the ecosystem of low biological heterogeneity, see Hestir et al., 2008 for example), but are commonly integrated over patches of vegetation.

Digital cameras have been applied to the ground-based phenological observations in recent years for their high accuracy and low labor

* Corresponding author. Tel.: +86 871 5160904.
E-mail address: yipingzh@xtbg.ac.cn (Y. Zhang).

1574-9541/$ – see front matter © 2012 Published by Elsevier B.V.
doi:10.1016/j.ecoinf.2012.03.001

cost (Ahrends et al., 2008, 2009; Crimmins and Crimmins, 2008; Ide and Oguma, 2010; Richardson et al., 2007, 2009). Indices based on the spectral information in red, green and red wavelengths were used to date phenological events. Furthermore, they also correlate well with the Normalized Difference Vegetation Index (NDVI, which is an index to indicate the status of vegetation), rate of canopy photosynthesis and gross primary production (GPP) (Ahrends et al., 2009; Richardson et al., 2007, 2009). In Japan, digital cameras were installed in 43 national parks to monitor the seasonal vegetation variation (Ide and Oguma, 2010). In their studies, daily digital images of the last 8 years were analyzed to estimate green-up dates of the vegetation. While the methodology was suggested to be a potential approach for a worldwide network of phenological observation, the technique is still far from mature. In former studies (Ahrends et al., 2008, 2009; Ide and Oguma, 2010; Richardson et al., 2007), only greenness indices were used to estimate the dates of green-related events (*e.g.*, leaf emergence and leaf green up), but senescence events (*e.g.*, leaf coloring and shedding) were seldom analyzed (but see Ahrends et al., 2009). Besides, the technique still needs to be validated with more species and ecosystems and under diverse environmental conditions.

In this study, images of three species (two from an evergreen broad-leaved forest and one from a seasonal rain forest) were used to estimate phenological events of leaf development and senescence. In addition to the greenness index used in former studies, a redness index was also employed. Our objectives were to: 1) evaluate the accuracy of the timing of phenological events from the two color indices, 2) compare it among the three tree species, and 3) reveal the effects of climatic factors on phenological events based on the color indices. Additionally, the effect of camera white balance setting on the day-to-day fluctuations of output data was also discussed.

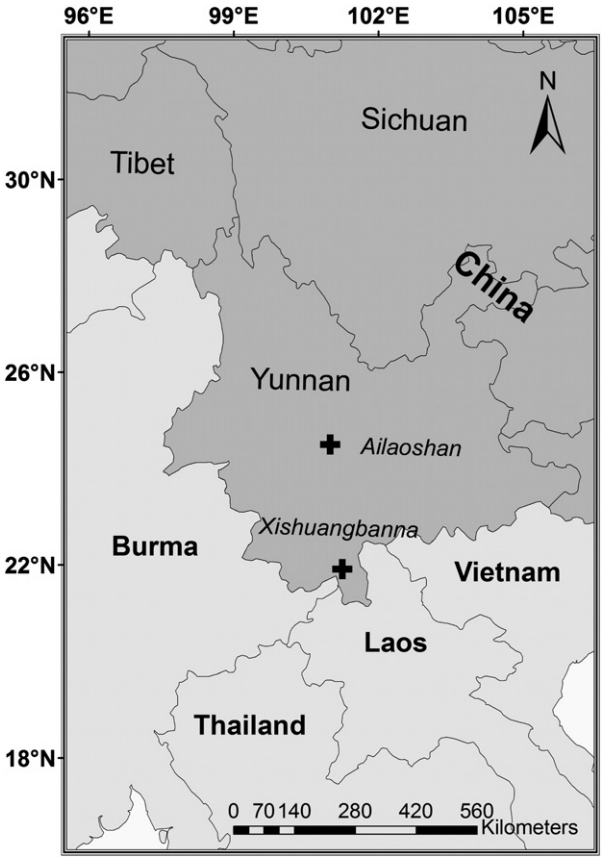

Fig. 1. The locations of the two study sites (black crosses).

2. Materials and methods

2.1. Study sites and materials

Study sites are located in Ailaoshan Mountain Nature Reserve (24°32′N, 101°01′E, 2476 masl) and Menglun Nature Reserve of Xishuangbanna (21°55′N, 101°15′E, 750 masl) in Yunnan Province, southwestern China (Fig. 1).

At Ailaoshan, it is covered with a subtropical evergreen broad-leaved forest with a canopy height of ~25 m. The annual mean temperature is 11.3 °C with an average annual precipitation of 1840 mm (Tan et al., 2010). Here we studied two species, *Machilus bombycina* (Lauraceae) and *Acer heptalobum* (Aceraceae). They are important components of the forest (Qiu, 1998) with different vegetative strategies (*i.e.*, *M. bombycina* is evergreen, while *A. heptalobum* is deciduous), and are within the reachable range of the camera view. A 34 m high steel tower was erected at the site for meteorological monitoring and carbon flux observation (Tan et al., 2010), and we installed a Ricoh Caplio R4 digital camera, which can take images automatically at given time intervals, at 30 m above ground on this tower, facing southwest. During the observation period, images were taken every 3 h and saved in JPEG format (2816×2112 pixels). The camera was operated in automatic exposure mode with the white balance adjustment in "automatic mode". We used midday images for analysis to avoid the effect of solar angles (Ahrends et al., 2008, 2009; Ide and Oguma, 2010). Images with raindrops on the lens, rain or heavy fog were excluded. We selected two fixed areas of interest (AOI), valid for each image for the whole monitoring period, as representatives for the canopies of *M. bombycina* and *A. heptalobum* (see Fig. 2). The observation period lasted from 1 January to 21 December 2010; however, images for the first twenty days are missing due to technical failures (Fig. 3).

At Xishuangbanna, the tropical seasonal rain forest is dominated by the deciduous species *Pometia tomentosa* (Sapindaceae), which was studied in this study, with a canopy height >30 m (Cao et al., 1996; Hu et al., 2010). Annual mean temperature is 21.7 °C with an annual precipitation of 1487 mm. There is a 70 m tower for meteorological monitoring and carbon flux observation within the site (Zhang et al., 2010). A southeast-facing Ricoh Caplio R4 digital camera was mounted at 36 m above ground. Camera setting, image capturing and picking process were the same as in Ailaoshan site, except for the white balance setting, which was fixed (in "outdoor mode"). In each image, a fixed AOI of *P. tomentosa* was selected for analysis (see Fig. 2). The observation period started on 1 January and lasted until 28 December 2010 (Fig. 4). During this period, images from 7 October to 6 November are missing due to technical failures.

Daily climatic data in 2010 from the meteorological towers in Ailaoshan and Xishuangbanna, including temperature, photosynthetic active radiation (PAR) and rainfall, were used to reveal the climatic effects on the phenology. In contrast to the complete data set from Ailaoshan, the temperature data of 18–22 April and 8–17 May, the PAR data of 12 May–22 June and 3–5 December as well as the rainfall data of 6–17 May and 13–22 June are missing in Xishuangbanna due to technical failures.

2.2. Data analysis

In the AOI of each image (Fig. 2), the color values (red, green and blue, referred to as R, G and B, respectively) were extracted from each pixel and averaged on a daily basis. Indices including red fraction (RF = R/(R + G + B)) and green fraction (GF) were introduced to normalize the value of R and G by instantaneous total brightness.

The color of the forest canopy was used to describe vegetative phenology, as it reflects the seasonal variation of vegetation (Ide and Oguma, 2010; Richardson et al., 2007, 2009). Three phenological events of leaf development and senescence were studied: (1) start of

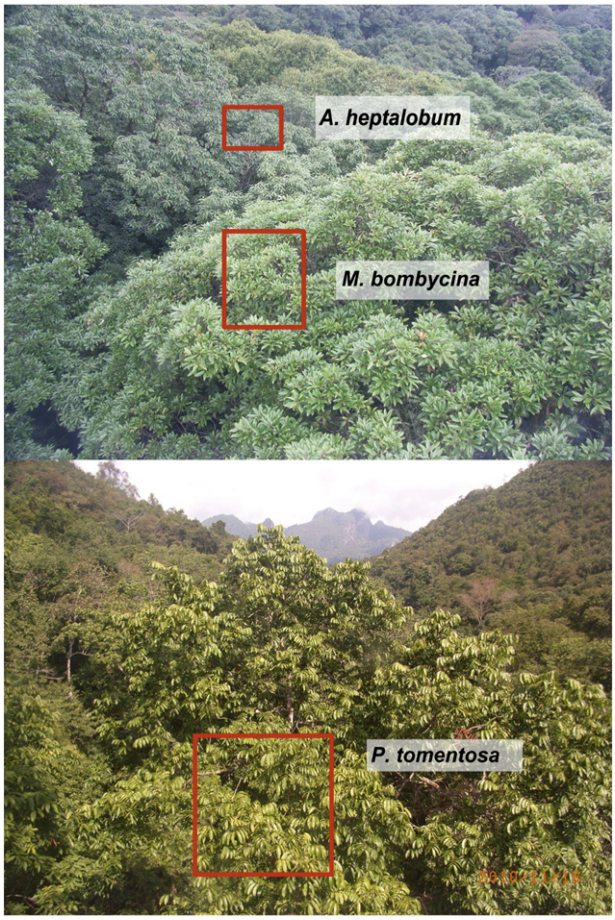

Fig. 2. Two sample images (taken on 15 June and 19 November 2010, respectively) showing the area of interest (AOI, see Section 2.1) for the 3 studied species in forests at Ailaoshan (upper panel) and Xishuangbanna (lower panel). AOI includes 24,897 pixels for *A. heptalobum*, 105,937 pixels for *M. bombycina* and 441,441 pixels for *P. tomentosa*.

growing season (SGS): leaves begin to appear; (2) start of leaf senescence (SLS): leaves begin to change color; (3) end of leaf senescence (ELS): the tree turns to be leafless. These events are commonly used in remote sensing and phenological studies (Ahrends et al., 2009; Zhang et al., 2003). During these periods, sigmoid curves were used to fit the RF and GF values (Fisher et al., 2006; Ide and Oguma, 2010; Richardson et al., 2007; Zhang et al., 2003):

$$y = a + \frac{b}{1 + e^{(c-dx)}}$$

where y represents the RF or GF values, x represents the day of year (DOY) and a to d are regression parameters estimated by least squares method (see Fig. 5 as example). The occurrence of the phenological event was determined as the DOY with a maximum absolute value of the second derivative of y (Ahrends et al., 2008, 2009; Ide and Oguma, 2010). We also visually assessed the dates of these events from the images to validate the estimated timing (Table 1).

To explore the effects of climate on each phenological event, we used RF or GF with the most accurate estimates (noted in bold in Table 1). For each of these phenological periods, a cross-correlation over a 30-day window was computed to detect the strength of relation and the time lags between RF or GF and climatic factors, with the assumption that variation of climatic factors leads the phenology.

For digital images, white appears to be different from what is recognized by the eyes under various light sources or conditions, which in turn impacts the color of all pixels. White balance is a calibration procedure to remove this color discrepancy. The "automatic white balance" mode available in digital cameras allows automatic adjustment to diverse light conditions. Many phenological studies with digital cameras suggested that the white balance of the cameras should be fixed in order to minimize the day-to-day fluctuations of the color index (Ahrends et al., 2008, 2009; Ide and Oguma, 2010). In this study, we investigated the difference between results from the images taken with automatic white balance (Ailaoshan) and with fixed white balance (Xishuangbanna). We assumed no differences in true leaf color between two successive days for the same tree and the observed variation in leaf color was caused by differences in the white balance setting and weather condition. Then, based on this assumption, a moving standard deviation (SD) for RF or GF was calculated for all two-day windows except during periods of phenological events with rapid changes in leaf color (DOY: 120–210 for *M. bombycina*, 30–150 and 260–355 for *A. heptalobum*, 30–180 for *P. tomentosa*). Each of the SD multiplies 1000 was deemed as a noise coefficient to represent the day-to-day fluctuation of RF or GF. To reveal differences among species, a nonparametric Mann–Whitney *U* test (because data series are non-normally distributed) was performed with RF and GF as factors and noise coefficients as dependent variables (Fig. 6). If a fixed white balance could effectively reduce the noise of RF or GF, the noise coefficients of *P. tomentosa* (fixed white balance) should be significantly lower than for the other two species with automatic white balance adjustment.

3. Result

3.1. Variations of RF and GF

At Ailaoshan, the two species showed different RF and GF variation patterns during the studied period (Fig. 3). For the evergreen species *M. bombycina*, only SGS was studied because there is no general leaf senescence period in evergreen species. GF varied only when SGS occurred in May, which might be induced by the increasing rainfall in April. GF dropped when yellow new leaves began to flush and increased only after leaves were fully developed and turned green. This GF pattern in *M. bombycina* is distinct from the other two species with green or red young leaves, whose GF or RF values increased as leaves flushed (see Figs. 3 and 4). In RF, no substantial shift occurred during SGS, indicating that RF is not sensitive enough to detect the appearance of the yellow young leaves.

RF and GF for the deciduous species *A. heptalobum* varied much more during the studied period than in *M. bombycina*, (Fig. 3). In the annual cycle, two peaks developed in RF and one peak in GF. Both RF and GF values increased simultaneously with SGS in March, but GF reached higher values than RF. This increase in RF and GF seems to be driven by the temperature rise in March. After leaves were fully developed, GF dropped to ~0.36 and remained until the end of October when SLS occurred. Leaf coloring (SLS) caused a decrease in GF to ~0.33 and an increase in RF to ~0.36. Finally, after ELS, RF also declined to ~0.33. Note that the value 0.33 is like a baseline for RF and GF, at which no substantial redness or greenness is presented in AOI of the images. In view of the annual pattern, RF appeared to be negatively related to temperature and rainfall.

At Xishuangbanna, the GF annual pattern of the deciduous species *P. tomentosa* showed one peak and RF exhibited two peaks (Fig. 4). All three phenological events occurred before May. Similar as in *A. heptalobum*, GF decreased and RF increased with the onset of SLS in February. At the end of March, the tree had turned leafless (ELS), and GF and RF had dropped to ~0.36 and ~0.41, respectively. Right after that, RF increased (but not GF) with the onset of SGS, because the developing leaves of *P. tomentosa* are red. GF only started to increase when some young leaves turned green one week after SGS. With respect to the environmental drivers, leaf senescence was

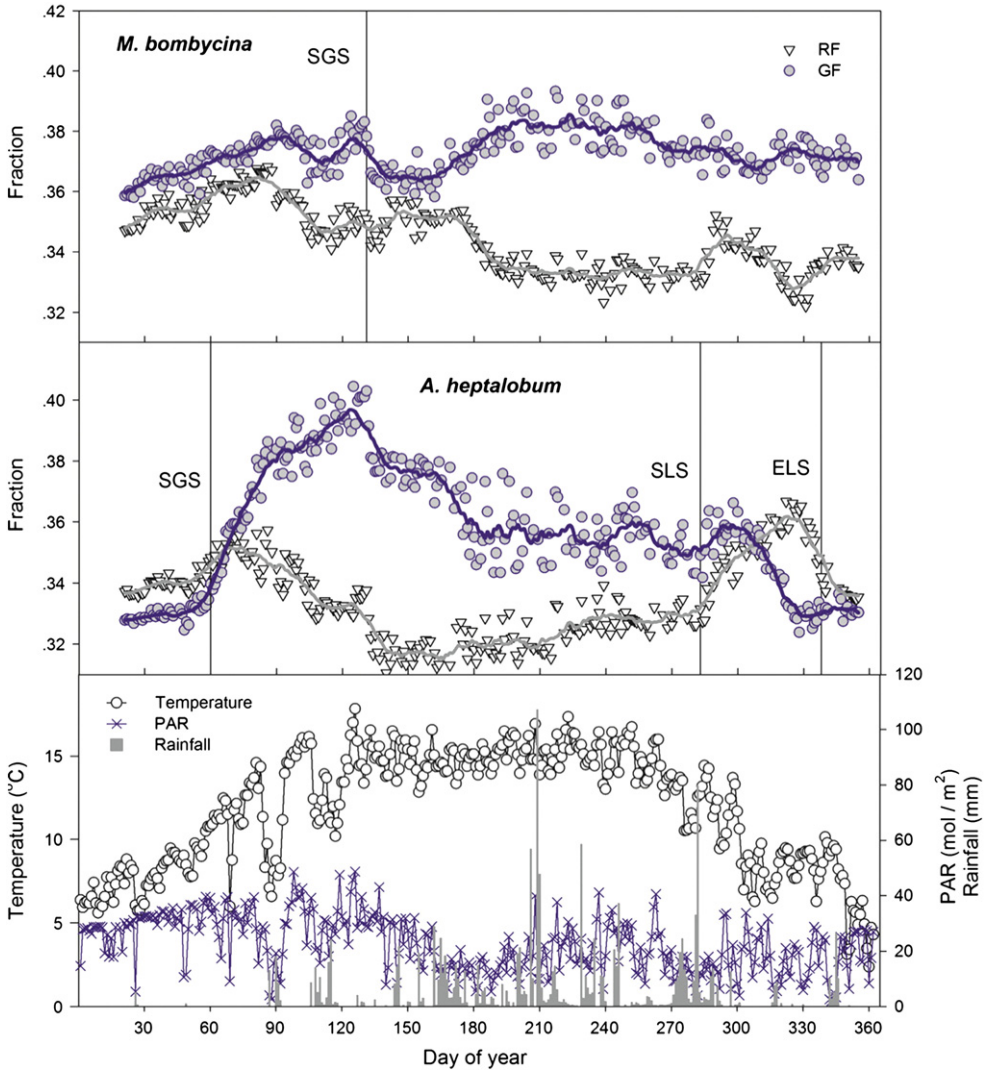

Fig. 3. Annual patterns of daily red fraction (RF) and green fraction (GF) derived from area of interest (see Fig. 2 and Section 2.2) for *M. bombycina* (top) and *A. heptalobum* (middle) and annual patterns of daily climatic factors in 2010 at Ailaoshan (bottom). The study period was from 21 January to 21 December 2010. Smooth lines of 15-window boxcar filter have been added to the RF and GF distributions to improve visualization of their annual patterns. Vertical lines indicate the occurrences of phenological events (SGS: start of growing season; SLS: start of leaf senescence; ELS: end of leaf senescence). Climatic factors include the temperature, photosynthetic active radiation (PAR) and rainfall.

probably driven by the absence of rainfall before April and leaf development by an increase in temperature and rainfall following SLS.

3.2. Estimated date for each phenological event

For each studied phenological event, estimated dates are quite different depending on whether they are based on RF or GF (see Fig. 5 and Table 1), and the absolute differences of the estimated dates ranged from −4 to 1 day and from −2 to 27 days, respectively (Table 1). In the phenophase of leaf development (SGS), regardless of the case in *P. tomentosa* whose young leaves are red, estimated dates from GF (absolute difference: −2 to 0 day) are more accurate than those from RF (absolute difference: −4 to 1 day). However, in the leaf senescence phase, estimated dates from RF (absolute difference: −3 to 1 day) are much more accurate than those from GF (absolute difference: 9 to 27 days). In the case of ELS, the dates can only be estimated by RF, because GF of the two studied deciduous species dropped to minimum when all leaves turned red before ELS and without obvious shift afterwards. In conclusion, events involving red leaves (*i.e.*, SLS, ELS and the SGS of *P. tomentosa*) can be estimated more accurately by RF while events characterized by green leaves (*i.e.*, SGS for *A. heptalobum* and *M. bombycina*) should be estimated by GF (see Table 1, noted in bold). Using this strategy, absolute differences of the estimated dates for all the phenological events remain within −3 to 1 days.

3.3. Impact of environmental factors

All RF or GF variations during the periods of phenological events showed significant correlations with climatic factors (Table 2). Phenological events occurred with an average time lag of 10 days to the climatic signals ranging from 0 to 25 days. These time lags are generally longer in *A. heptalobum* than the other two species, indicating a slower response of *A. heptalobum* to environmental changes. Temperature is the key factor for all three events in the three species. PAR is also a dominant driving factor for events in *P. tomentosa* at Xishuangbanna. By contrast, rainfall showed less impact on most events (except for the case of SGS in *A. heptalobum* and *M. bombycina* at Ailaoshan).

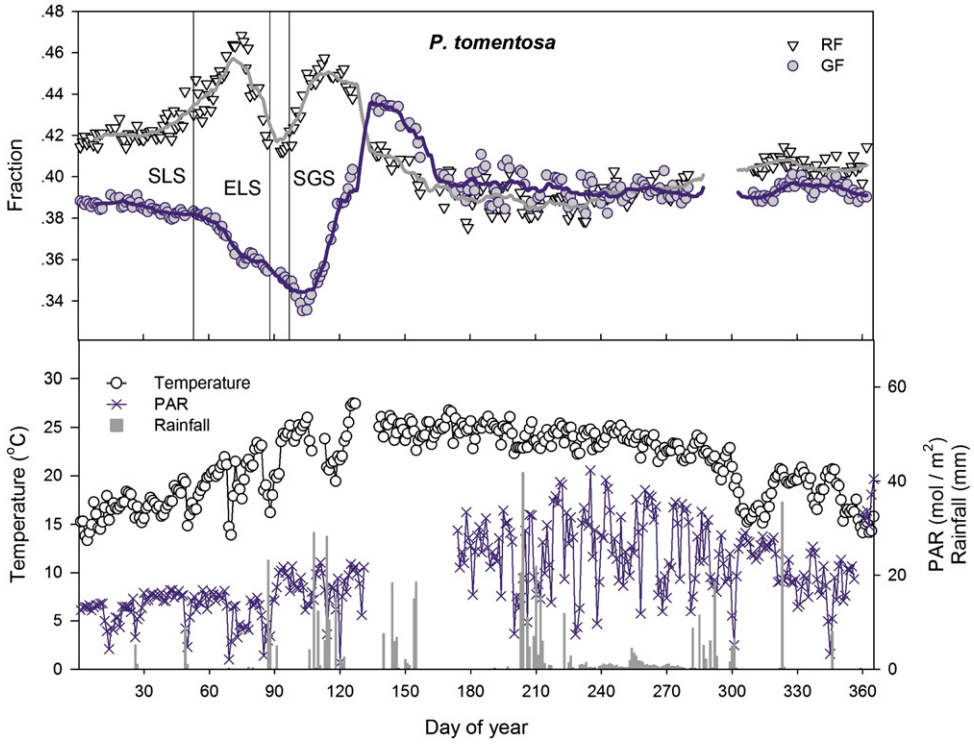

Fig. 4. Annual patterns of daily red fraction (RF) and green fraction (GF) derived from area of interest (see Fig. 2 and Section 2.2) for *P. tomentosa* (upper panel) and annual patterns of daily climatic factors in 2010 at Xishuangbanna (lower panel). The study period was from 1 January to 28 December 2010. Smooth lines of 15-window boxcar filter have been added to the RF and GF distributions to improve visualization of their annual patterns. Vertical lines indicate the occurrences of phenological events (SGS: start of growing season; SLS: start of leaf senescence; ELS: end of leaf senescence). Climatic factors include the temperature, photosynthetic active radiation (PAR) and rainfall.

4. Discussion

4.1. Accuracy of the estimated timing for each phenological event

The primary purpose of this study was to evaluate the accuracy of the estimated dates of phenological events from digital images. Two study sites with different forest types were included because different conditions in different forest types may influence the timing of phenological events from digital images. Estimates from digital cameras showed a high accuracy (absolute difference: −3 to 1 day, see Table 1) in monitoring the phenology of the three different species. Former studies have demonstrated the feasibility of observing phenology with digital cameras for the species in temperate regions (Ahrends et al., 2008; Ide and Oguma, 2010; Richardson et al., 2007). However, when estimating the events of leaf senescence with greenness index, higher discrepancies were found (Ahrends et al., 2009), which is why the redness index was introduced in this study.

For the three studied species, different patterns between RF and GF variation were shown in all the phenological events (Figs. 3 and 4), which resulted in different estimated dates from them (Table 1). Generally, to achieve higher accuracy, events associated with red leaves (SLS, ELS and the SGS for *P. tomentosa*) should be estimated by RF, while events related to the green leaves (SGS for *A. heptalobum*

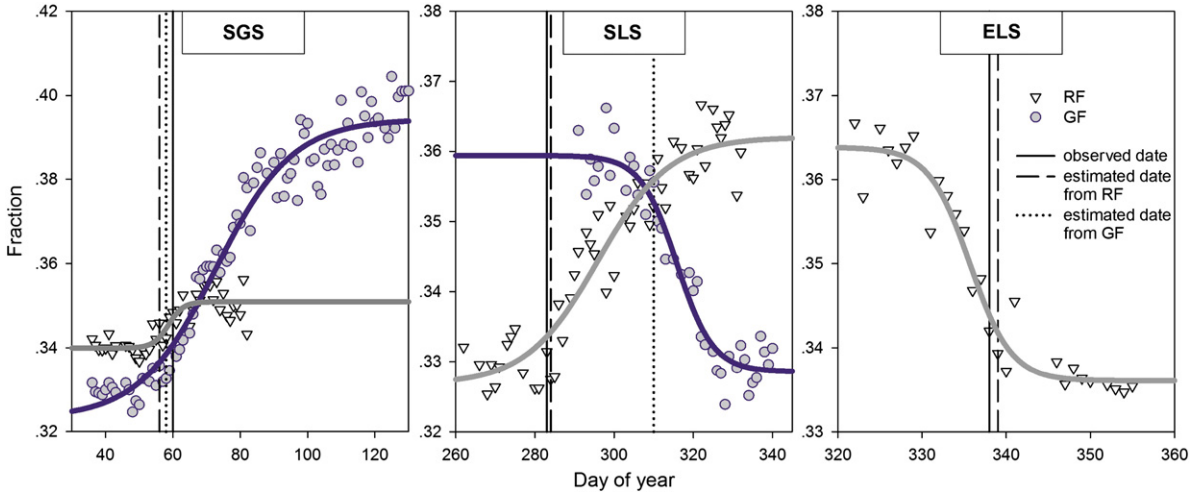

Fig. 5. Example of sigmoid regressions for estimating the time of phenological event in *A. heptalobum* (SGS: start of growing season; SLS: start of leaf senescence; ELS: end of leaf senescence). Vertical solid lines denote observed dates of the events from images. Vertical dashed lines and dotted lines denote the estimated dates from red fraction (RF) and green fraction (GF), respectively (see Section 2.2). GF was not used for timing of ELS because it dropped to the minimum when all leaves turned red before ELS occurred.

Table 1
Dates of phenological events for the 3 studied species showing the observed dates (Obs), estimated dates (Est) derived from red fraction (RF) and green fraction (GF) and the absolute differences (Diff) between the estimated dates and observed dates. "–" denotes that no substantial change of RF or GF occurred around the events. SGS: start of growing season; SLS: start of leaf senescence; ELS: end of leaf senescence. Fraction (RF or GF) with the more accurate estimated date for each event is noted in bold. All dates are in the form of DOY (day of year).

Site/species	Event	Obs	Est			
			RF	Diff	GF	Diff
Ailaoshan						
A. heptalobum	SGS	60	56	−4	**58**	**−2**
	SLS	283	**284**	**1**	310	27
	ELS	338	**339**	**1**	–	–
M. bombycina	SGS	131	–	–	**131**	**0**
Xishuangbanna						
P. tomentosa	SGS	97	**98**	**1**	115	18
	SLS	53	**51**	**−2**	62	9
	ELS	88	**85**	**−3**	–	–

and *M. bombycina*) should be estimated by GF (noted in bold in Table 1). Using this strategy, the timing accuracy was much improved from the estimates only from GF, especially for the events of leaf senescence (SLS and ELS). The greenness index was not sensitive enough to reflect the color variation of the leaves when they turn into colors other than green (*e.g.*, red) because the greenness can totally vanish. Therefore, it is suggested to include a redness index when estimating the phenology of the species whose leaf color is periodically red (*e.g.*, some deciduous species).

With the introduction of the redness index, the technique of phenological estimation with digital images has been much improved. Not only can the event of leaf development be accurately estimated from it, but also the events of leaf senescence. Further, based on this improvement, the technique is expected to be applied to more species in different forest types.

4.2. Impacts of the climatic factors

Climatic factors were well correlated with the RF or GF and showed a average time lag of 10 days during periods of phenological events (Table 2), indicating that it is possible to reveal the climatic impacts on phenology. Studies with long-term inter-annual data suggested that the time lag of plant phenology varies from a few days to several months, which is a period for temperature accumulation or leaf development preparation (Cannell and Smith, 1983; Chuine, 2000; Doi and Katano, 2008; Gordo and Sanz, 2010). However, in this study, the cross-correlation was computed only over a 30-day window, because our data had a daily resolution and it seems unreliable to estimate a time lag of several months without long-term inter-annual data. Therefore, the lags here represent the delay of phenological responses, but may not relate to the mechanisms of plant development.

After all, to determine the impact of environmental drivers on phenological events within a year, daily data from digital camera are more effective than conventional observed records, which include only the dates of occurrence for the events. With long-term daily data of canopy color, it is possible to analyze the phenological responses to inter-annual climate change, and it can also reflect the change of forest NDVI, photosynthesis rate and GPP (Ahrends et al., 2009; Richardson et al., 2007, 2009).

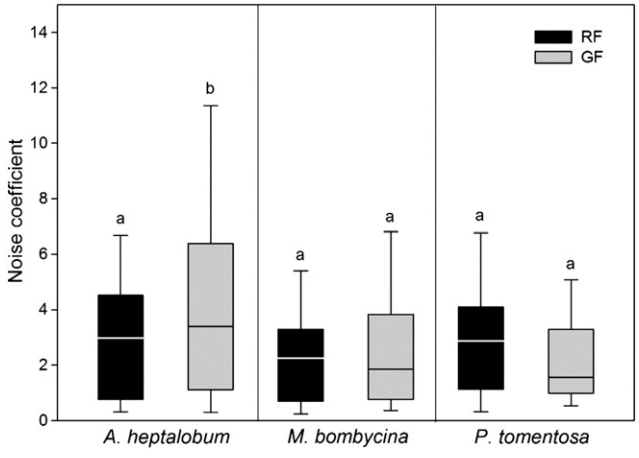

Fig. 6. Noise coefficients of red fraction (RF) and green fraction (GF) for the 3 studied species. Images of *P. tomentosa* were corrected with a fixed white balance while images of *A. heptalobum* and *M. bombycina* were taken in an automatic white balance mode. Mann–Whitney *U* test was performed with RF and GF as factors and noise coefficients as dependent variables. Different letters indicate significant differences ($p<0.05$). The bottom and top of a box indicate the values of lower and upper quartiles, respectively, and the horizontal line within the box is the median. The lower and upper whiskers represent the values of the 10th and 90th percentiles, respectively.

4.3. Day-to-day noise for RF and GF

Day-to-day fluctuations (noise) of RF and GF were observed during the studied period for the three species (Figs. 3, 4). Some studies suggested using a fixed white balance setting to minimize this noise (Ahrends et al., 2008, 2009; Ide and Oguma, 2010). In this study, the camera at Ailaoshan (*A. heptalobum* and *M. bombycina*) was set in an automatic white balance mode while it was in fixed mode at Xishuangbanna (*P. tomentosa*). This allowed us to explore the impacts of white balance setting on the quality of the output data.

Result showed (Fig. 6) that the noise coefficients of RF and GF in the case of *P. tomentosa* (fixed white balance) are not necessarily lower than those in the other two species (automatic white balance). This means that the impacts of the white balance setting were not the main cause of day-to-day noise and a fixed white balance could not effectively reduce the noise of output data. The noise may have been mainly induced by fog and atmospheric conditions. In the case of the GF of *A. heptalobum*, the noise coefficients are significantly higher than in other cases, owning to the long distance from the camera to the canopy of the tree (Fig. 2). A longer distance may include more fog and enhance the distortion of colors in the images. However, noise coefficients are not higher in RF, suggesting that greenness indices can be more easily impacted by the distance than redness indices. After all, to get high-quality images, a proper distance should be set between the camera and sample trees.

4.4. Implications of digital camera monitoring

Digital camera monitoring, for its high accuracy in phenology observation, is an alternative option to replace the conventional phenology observation and bridges the gap between remote sensing data from satellites and field observations. Compared with the conventional observation, this technique requires fewer volunteers, which makes long-term standardized observations at widely distributed study sites possible, even in some remote areas. Furthermore, phenological networks of regional or even global scale might be established with the support of this technique (Ide and Oguma, 2010).

Despite the advantages of the technique, some limitations also appeared. First, missing data may occur occasionally due to technical failure or weather condition. The missing data during periods of phenological events can directly induce discrepancies in estimated dates. Hence we recommend taking additional conventional observations during bad weather conditions, especially during the

Table 2
Cross-correlation coefficients between red fraction (RF) or green fraction (GF) of each phenological event and climatic factors. Only the fraction (RF or GF) with a more accurate estimated date is presented for each event (see Table 1). RP: the representative period of each event, within which the data are used in the cross-correlation, and it is presented in the form of DOY (day of the year). Lag: the time lag that gives the maximum absolute value of cross-correlation coefficient for each event. R: maximum/minimum cross-correlation coefficient. SGS: start of growing season; SLS: start of leaf senescence; ELS: end of leaf senescence.

Species	Event	Fraction	RP	Temperature		PAR		Rainfall	
				Lag	R	Lag	R	Lag	R
A. heptalobum	SGS	GF	30–130	22	0.775^{***}		NS	15	0.350^{***}
	SLS	RF	260–330	15	-0.850^{***}	25	-0.420^{**}	0	-0.433^{**}
	ELS	RF	320–355	0	0.545^{**}	23	0.507^{**}		NS
M. bombycina	SGS	GF	120–160	13	-0.747^{***}	4	0.492^{**}	16	0.530^{***}
P. tomentosa	SGS	RF	90–120	8	0.919^{***}	10	0.740^{***}		NS
	SLS	RF	20–80	4	0.700^{***}	0	-0.455^{***}		NS
	ELS	RF	70–100	2	-0.657^{***}	3	-0.702^{***}	16	-0.432^{*}

Significant levels: ***, $p<0.001$; **, $p<0.01$; *, $p<0.05$; NS, not significant ($p>0.05$).

onset of phenological transitions. Another problem is that the color change of the images is still not sensitive enough to detect flowers and fruits of the studied trees. Although it may be possible to estimate the dates of reproductive events for some species with flowers or fruits of conspicuous size and color or with higher resolution cameras or large zoom lens, which still needs to be verified, conventional observation is still suggested in reproductive phenology studies.

Besides phenological observations, digital images of the canopy with daily resolution offer potential opportunities for improving the simulation and prediction of dynamic processes in forests (*e.g.*, carbon flux or transpiration modeling). Moreover, to estimate the vegetation variation of the forest, more trees should be included in the visual field of the cameras at a proper distance. For this purpose, we recommend setting up more than one camera and facing different directions to cover more areas of the forest. Additionally, a comparison between data from camera images and satellite images should be carried out in the future, which may provide a way to validate the result from satellite remote sensing.

5. Conclusions

To accurately estimate the dates of phenological events from digital images, both the greenness and redness indices are needed. In this study, variations of the color indices (RF or GF) during periods of phenological events were well correlated with climatic factors and showed a time lag of around 10 days. With respect to the camera setting, the automatic white balance mode does not necessarily increase the day-to-day noise of the output data compared to a fixed white balance. Instead, the quality of the data is more affected by the weather condition and the distance from camera to the canopy of the tree. Because of its convenience (*i.e.*, automatic sampling, low labor cost), data from digital images provide a possible and efficient mean for the future ecosystem process modeling, phenological networks establishing and remote sensing validating.

Acknowledgments

We thank Mr. Deng Yun for collecting the digital images. We are grateful to Dr. Henrik Hartmann and Dr. Wu Xiuchen in Max Planck Institute for Biogeochemistry, Germany, for the linguistic help and providing the figure of geographic locations of the study sites, respectively. This study was supported by the National Natural Science Foundation of China (30670395, 31061140359, 41071071 and 41001063), the Knowledge Innovation Program of the Chinese Academy of Sciences (KSCX2-YW-Z-004 and KZCX2-YW-Q1-05-04), and the Yunnan Natural Science Foundation of Yunnan Province, China (2004C0053M).

References

Ahl, D.E., Gower, S.T., Burrows, S.N., Shabanov, N.V., Myneni, R.B., Knyazikhin, Y., 2006. Monitoring spring canopy phenology of a deciduous broadleaf forest using MODIS. Remote Sensing of Environment 104, 88–95.
Ahrends, H.E., Brugger, R., Stockli, R., Schenk, J., Michna, P., Jeanneret, F., Wanner, H., Eugster, W., 2008. Quantitative phenological observations of a mixed beech forest in northern Switzerland with digital photography. Journal of Geophysical Research 113. doi:10.1029/2007JG000650.
Ahrends, H.E., Etzold, S., Kutsch, W.L., Stoeckli, R., Bruegger, R., Jeanneret, F., Wanner, H., Buchmann, N., Eugster, W., 2009. Tree phenology and carbon dioxide fluxes: use of digital photography at for process-based interpretation the ecosystem scale. Climate Research 39, 261–274.
Bradshaw, W.E., Holzapfel, C.M., 2008. Genetic response to rapid climate change: it's seasonal timing that matters. Molecular Ecology 17, 157–166.
Cannell, M., Smith, R., 1983. Thermal time, chill days and prediction of budburst in *Picea sitchensis*. Journal of Applied Ecology 951–963.
Cao, M., Zhang, J., Feng, Z., Deng, J., Deng, X., 1996. Tree species composition of a seasonal rain forest in Xishuangbanna, Southwest China. Tropical Ecology 37, 183–192.
Chen, X., Hu, B., Yu, R., 2005. Spatial and temporal variation of phenological growing season and climate change impacts in temperate eastern China. Global Change Biology 11, 1118–1130.
Chiang, J.M., Brown, K.J., 2007. Improving the budburst phenology subroutine in the forest carbon model PnET. Ecological Modelling 205, 515–526.
Chuine, I., 2000. A unified model for budburst of trees. Journal of Theoretical Biology 207, 337–347.
Crimmins, M.A., Crimmins, T.M., 2008. Monitoring plant phenology using digital repeat photography. Environmental Management 41, 949–958.
Doi, H., Katano, I., 2008. Phenological timings of leaf budburst with climate change in Japan. Agricultural and Forest Meteorology 148, 512–516.
Fisher, J.I., Mustard, J.F., Vadeboncoeur, M.A., 2006. Green leaf phenology at Landsat resolution: scaling from the field to the satellite. Remote Sensing of Environment 100, 265–279.
Fitzjarrald, D.R., Acevedo, O.C., Moore, K.E., 2001. Climatic consequences of leaf presence in the eastern United States. Journal of Climate 14, 598–614.
Gordo, O., Sanz, J.J., 2009. Long-term temporal changes of plant phenology in the Western Mediterranean. Global Change Biology 15, 1930–1948.
Gordo, O., Sanz, J.J., 2010. Impact of climate change on plant phenology in Mediterranean ecosystems. Global Change Biology 16, 1082–1106.
Hestir, E.L., Khanna, S., Andrew, M.E., Santos, M.J., Viers, J.H., Greenberg, J.A., Rajapakse, S.S., Ustin, S.L., 2008. Identification of invasive vegetation using hyperspectral remote sensing in the California Delta ecosystem. Remote Sensing of Environment 112, 4034–4047.
Hu, Y., Cao, M., Lin, L., 2010. Dynamics of tree species composition and community structure of a tropical seasonal rain forest in Xishuangbanna, Southwest China. Acta Ecologica Sinica 30, 949–957 (in Chinese).
Ide, R., Oguma, H., 2010. Use of digital cameras for phenological observations. Ecological Informatics 5, 339–347.
Keatley, M.R., Fletcher, T.D., Hudson, I.L., Ades, P.K., 2002. Phenological studies in Australia: potential application in historical and future climate analysis. International Journal of Climatology 22, 1769–1780.
Keeling, C.D., Chin, J.F.S., Whorf, T.P., 1996. Increased activity of northern vegetation inferred from atmospheric CO_2 measurements. Nature 382, 146–149.
Kharin, N., 1976. Mathematical models in phenology. Journal of Biogeography 3, 357–364.
Kington, J., 1974. An application of phenological data to historical climatology. Weather 29, 320–328.
Matsumoto, K., Ohta, T., Irasawa, M., Nakamura, T., 2003. Climate change and extension of the *Ginkgo biloba* L. growing season in Japan. Global Change Biology 9, 1634–1642.

Menzel, A., 2002. Phenology: its importance to the global change community — an editorial comment. Climatic Change 54, 379–385.
Menzel, A., Fabian, P., 1999. Growing season extended in Europe. Nature 397, 659.
Niemand, C., Köstner, B., Prasse, H., Grünwald, T., Bernhofer, C., 2005. Relating tree phenology with annual carbon fluxes at Tharandt forest. Meteorologische Zeitschrift 14, 197–202.
Obrist, D., Verburg, P.S.J., Young, M.H., Coleman, J.S., Schorran, D.E., Arnone, J.A., 2003. Quantifying the effects of phenology on ecosystem evapotranspiration in planted grassland mesocosms using EcoCELL technology. Agricultural and Forest Meteorology 118, 173–183.
Penuelas, J., Filella, I., 2001. Phenology — responses to a warming world. Science 294, 793–795.
Qiu, X., 1998. Studies on the Forest Ecosystem in Ailao Mountains Yunnan, China. Yunnan Science and Technology Press, Kunming. (in Chinese).
Richardson, A.D., Jenkins, J.P., Braswell, B.H., Hollinger, D.Y., Ollinger, S.V., Smith, M.L., 2007. Use of digital webcam images to track spring green-up in a deciduous broadleaf forest. Oecologia 152, 323–334.
Richardson, A.D., Braswell, B.H., Hollinger, D.Y., Jenkins, J.P., Ollinger, S.V., 2009. Near-surface remote sensing of spatial and temporal variation in canopy phenology. Ecological Applications 19, 1417–1428.
Root, T.L., Price, J.T., Hall, K.R., Schneider, S.H., Rosenzweig, C., Pounds, J.A., 2003. Fingerprints of global warming on wild animals and plants. Nature 421, 57–60.
Rutishauser, T., Luterbacher, J., Jeanneret, F., Pfister, C., Wanner, H., 2007. A phenology-based reconstruction of interannual changes in past spring seasons. Journal of Geophysical Research 112. doi:10.1029/2006JG000382.
Schwartz, M., 1990. Detecting the onset of spring: a possible application of phenological models. Climate Research 1, 23–29.
Stockli, R., Studer, S., Appenzeller, C., Vidale, P.L., 2007. A comparative study of satellite and ground-based phenology. International Journal of Biometeorology 51, 405–414.
Tan, Z.H., Zhang, Y.P., Schaefer, D., Yu, G.R., Liang, N., Song, Q.H., 2010. An old-growth subtropical Asian evergreen forest as a large carbon sink. Atmospheric Environment 45, 1548–1554.
Walther, G.R., Post, E., Convey, P., Menzel, A., Parmesan, C., Beebee, T.J., Fromentin, J.M., Hoegh-Guldberg, O., Bairlein, F., 2002. Ecological responses to recent climate change. Nature 416, 389–395.
Zhang, X.Y., Friedl, M.A., Schaaf, C.B., Strahler, A.H., Hodges, J.C.F., Gao, F., Reed, B.C., Huete, A., 2003. Monitoring vegetation phenology using MODIS. Remote Sensing of Environment 84, 471–475.
Zhang, X.Y., Friedl, M.A., Schaaf, C.B., 2006. Global vegetation phenology from Moderate Resolution Imaging Spectroradiometer (MODIS): evaluation of global patterns and comparison with in situ measurements. Journal of Geophysical Research, Biogeosciences 111. doi:10.1029/2006JG000217.
Zhang, Y.P., Tan, Z.H., Song, Q.H., Yu, G.R., Sun, X.M., 2010. Respiration controls the unexpected seasonal pattern of carbon flux in an Asian tropical rain forest. Atmospheric Environment 44, 3886–3893.